Phase Diagram for the Collective Behavior of Limit-Cycle Oscillators

Paul C. Matthews[(a)] and Steven H. Strogatz
Department of Mathematics, Massachusetts Institute of Technology, Cambridge, Massachusetts 02139
(Received 26 March 1990)

We analyze a large dynamical system of limit-cycle oscillators with mean-field coupling and randomly distributed natural frequencies. Depending on the choice of coupling strength and the spread of natural frequencies, the system exhibits frequency locking, amplitude death, and incoherence, as well as novel unsteady behavior characterized by periodic, quasiperiodic, or chaotic evolution of the system's order parameter. The phase boundaries between several of these states are obtained analytically.

PACS numbers: 05.45.+b, 87.10.+e

Coupled nonlinear oscillators are of interest in both biology[1,2] and physics.[3-13] This Letter was motivated by a remarkable biological phenomenon known as collective synchronization.[1] Populations of biological oscillators can spontaneously synchronize to a common frequency, even if there is a distribution of natural frequencies across the population. Examples include swarms of fireflies that flash in synchrony, crickets that chirp in unison, synchronous firing of cardiac pacemaker cells, and groups of women whose menstrual cycles become synchronized.[2]

The onset of synchronization is like a phase transition: When the coupling between the oscillators exceeds a critical value, the system spontaneously changes from an incoherent to a synchronized state. This novel cooperative phenomenon has recently attracted a great deal of attention.[3-12] The essentials of the problem are (i) the microscopic subunits are limit-cycle oscillators, and (ii) the frequencies of the oscillators are distributed across the population. To simplify the analysis, most (though not all[5,6]) authors have considered mean-field models in which each oscillator is coupled equally to all the others.[1,3,4,7-11] Previous analyses have been restricted to the cases of strong coupling[7-10] or very weak coupling.[1,3,4] In both cases, the system was found to evolve to a statistical steady state, characterized by a stationary number density in phase space and a constant order parameter.

In this Letter we describe several new forms of collective behavior for limit-cycle oscillators, all of which occur for intermediate values of the coupling strength. These new kinds of behavior are *unsteady*, and include periodic, quasiperiodic, and chaotic motion of the order parameter. We also derive analytical expressions for the boundaries of the steady regions in the phase diagram. These analytical results generalize earlier results obtained in the limits of weak or strong coupling.

We consider a model[7-10] of linearly coupled oscillators, each near a Hopf bifurcation:

$$\dot{z}_j = z_j(1-|z_j|^2+i\omega_j) + \frac{K}{N}\sum_{i=1}^{N}(z_i - z_j)\,, \qquad (1)$$

for $j=1,\ldots,N$. Here $z_j(t)$ is the position of the jth oscillator in the complex plane, $K \geq 0$ is the coupling strength, and the frequencies ω_j are randomly chosen from a symmetric unimodal distribution $g(\omega)$ whose width is characterized by a parameter γ. We assume that the mean of $g(\omega)$ is zero, by using a rotating frame if necessary. In the absence of coupling, each oscillator has a stable circular limit cycle $|z_j|=1$. Our goal is to determine the long-term behavior of (1) for large N, as a function of K and γ.

We first describe our numerical simulations. Equation (1) was integrated numerically using 800 oscillators. The frequencies ω_j were chosen to be evenly spaced in the interval $[-\gamma,\gamma]$, corresponding to a uniform density $g(\omega)=1/2\gamma$ for $|\omega| \leq \gamma$, and $g(\omega)=0$ otherwise. Typically the long-term behavior of the system was independent of the initial conditions, except for two very thin hysteretic regions in K-γ space; these are discussed below.

The results are conveniently described in terms of a complex order parameter[1,3,7,8]

$$Re^{i\phi} = \frac{1}{N}\sum_{j=1}^{N} z_j\,, \qquad (2)$$

whose amplitude R measures the degree of collective synchronization. Figure 1 plots the evolution of R for increasing values of γ at fixed K. For small γ the system spontaneously synchronizes [Fig. 1(a)]. As γ is increased, $R(t)$ exhibits large oscillations [Fig. 1(b)], and then irregular oscillations [Fig. 1(c)]. For sufficiently large γ, the system approaches an incoherent state with R near 0 and all the oscillators running at their natural frequencies [Fig. 1(d)].

Figure 2(a) plots the long-term behavior of the system as a function of K and γ. In order of increasing complexity, the different types of behavior are the following. *Amplitude death*: Each oscillator has zero amplitude; the fixed point $z_j=0$ is stable. *Locking*: There is a stable fixed point of (1) with $R>0$, as in Fig. 1(a). The phase ϕ of (2) is arbitrary because Eq. (1) is rotationally symmetric. In the original frame where the mean of $g(\omega)$ is not zero, this solution corresponds to frequency locking, with the oscillators rotating rigidly about the origin at the mean frequency. *Incoherence*: Each oscillator moves at its natural frequency along a common cir-

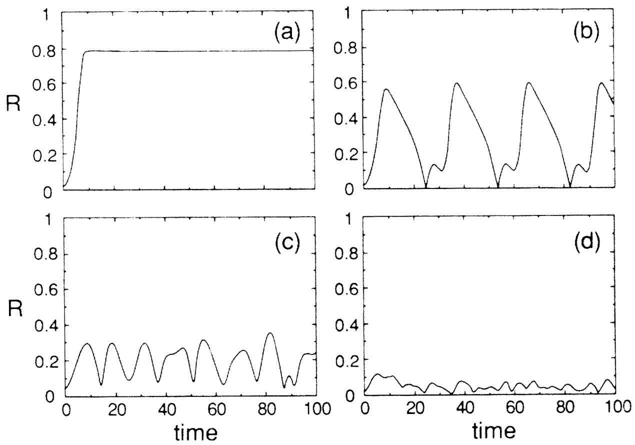

FIG. 1. Evolution of the amplitude R of the order parameter (2). Equation (1) was integrated for $K=0.8$ with the oscillators starting from random initial conditions in the square $|x| \leq 1$, $|y| \leq 1$. (a) $\gamma=0.6$, (b) $\gamma=0.8$, (c) $\gamma=1.0$, and (d) $\gamma=1.2$.

cle of radius $(1-K)^{1/2}$ centered on the origin. $R(t)$ has a constant value $R=0$. Strictly speaking, this solution exists only for infinite N; for large N the fluctuations in $R(t)$ are $O(N^{-1/2})$, as in Fig. 1(d).

In the death, locking, and incoherent regions, $R(t)$ always approaches a constant as $t \to \infty$. Such steady behavior has been reported previously.[3,7,8] The remaining region of the phase diagram is novel; it corresponds to *unsteady* motion of the order parameter.

Figure 2(b) shows the upper portion of the unsteady region. An enormous variety of behavior was uncovered in our numerical simulations; only the largest regions are shown in Fig. 2(b). *Hopf oscillations*: When $K>1$ the locked state loses stability via a Hopf bifurcation, leading to small quasisinusoidal oscillations about the locked state. *Large oscillations*: When $K<1$, the locked state undergoes a saddle-node bifurcation to large-amplitude oscillations, in which the order parameter (2) crosses through the origin along a line of constant ϕ, and hence $R(t)$ oscillates between 0 and large values, as in Fig. 1(b). *Quasiperiodicity*: The large oscillations lose stability via Hopf bifurcations, which add a second and then a third frequency to the system. *Chaos*: $R(t)$ is irregular [Fig. 1(c)] as is the phase $\phi(t)$. Numerical evidence suggests that this irregular motion is chaotic. First, there is a positive Lyapunov exponent: two slightly different initial conditions diverge exponentially fast. In contrast, this exponential divergence was not observed in the incoherent or quasiperiodic regions. Second, the time series of the real part of (2) has a broadband power spectrum with a roughly $1/f$ structure, whereas in the incoherent region, the power spectrum is flat for $|\omega| \leq \gamma$ and then falls off rapidly. For K near 1, the transition between chaos and incoherence is subcritical; there is a thin hysteresis region of width $\Delta\gamma \approx 0.01$ in which both

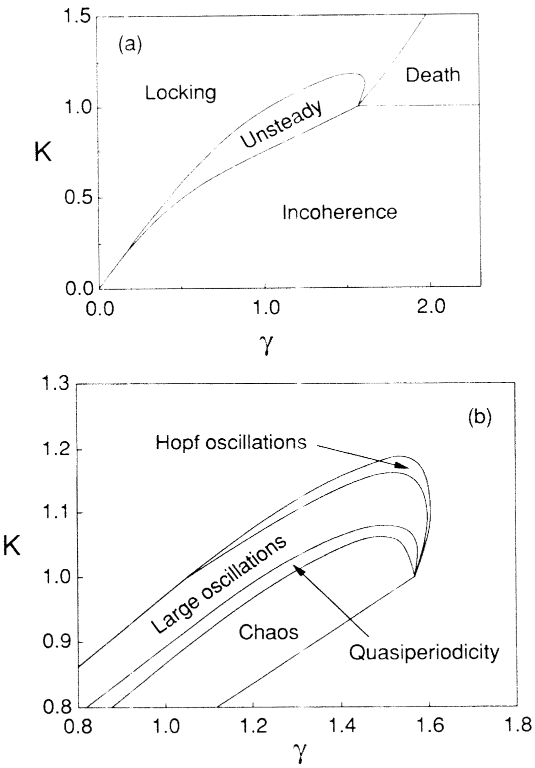

FIG. 2. (a) Phase diagram for Eq. (1) with frequencies uniformly distributed on $[-\gamma,\gamma]$. Locking-unsteady boundary determined numerically; other boundaries determined analytically. (b) Detail of the unsteady region in (a). All boundaries obtained numerically.

chaos and incoherence are locally stable. There is a second very thin hysteretic region (near $K=0.5$, $\gamma=0.43$, of width $\Delta\gamma \approx 0.001$) in which a periodic attractor coexists with the locked state. As γ increases through this region the system follows a period-doubling route to chaos.

We now outline our analytical calculations of the boundaries of the steady regions corresponding to amplitude death, locking, and incoherence. All calculations are for $N \to \infty$. The boundaries for both amplitude death and locking can be calculated at the same time because both states correspond to fixed points of Eq. (1). One can show that amplitude death is the only fixed point with $R=0$; henceforth we suppose $R>0$. By a rotation of coordinates, we may set $\phi=0$ in (2). Let $z_j = r_j \exp(i\theta_j)$. Then (1) becomes

$$\dot{\theta} = \omega - (KR/r)\sin\theta, \tag{3a}$$

$$\dot{r} = r(1-K-r^2) + KR\cos\theta, \tag{3b}$$

where the oscillators are now indexed by ω instead of j. Thus, a fixed point satisfies $\omega = (KR/r)\sin\theta$, $r(r^2+K-1) = KR\cos\theta$, and hence

$$(KR\sin\theta)^2 = \omega^2(1-K+\omega\cot\theta). \tag{4}$$

Fixed points must also satisfy the self-consistency equation

$$R=\int_{-\infty}^{\infty} r\cos\theta\, g(\omega)\,d\omega\,. \tag{5}$$

To determine the stability of a fixed point in the infinite-N limit, we must consider both the discrete and the continuous spectrum of the linearization of (1). We find[11] the following pair of equations for the discrete spectrum:

$$K^{-1}=\int_{-\infty}^{\infty}\frac{\lambda+2r^2+K-1\pm \mathrm{Re}(z^2)}{(\lambda+2r^2+K-1)^2+\omega^2-r^4}\,g(\omega)\,d\omega\,, \tag{6}$$

where $z=re^{i\theta}$ is the fixed point and λ is an eigenvalue. The plus and minus signs in (6) arise from collective modes associated with angular and radial motions of the order parameter, respectively. When the plus sign is chosen, Eq. (6) is satisfied *identically* by $\lambda=$ this reflects the rotational symmetry of the original system (1). The continuous spectrum[10,11] is given by $\lambda=1-K-2r^2\pm(r^4-\omega^2)^{1/2}$, and is associated with perturbations of a single oscillator while the others remain fixed. Thus, a fixed point may lose stability in three qualitatively different ways.

The boundary of the amplitude-death region may now be found by setting $z=r=0$. Then (6) has at most one solution λ and it is necessarily real.[10] Stability is lost when $\lambda=0$; for a uniform $g(\omega)$ the integral in (6) then yields $\tan(\gamma/K)=\gamma/(K-1)$. Equivalent results for this part of the death boundary have been found previously.[8,9] The continuous spectrum is $\lambda=1-K+i\omega$, where ω runs over the support of $g(\omega)$. Hence $K>1$ is also needed for stability. The death region has a corner at the point $K=1$, $\gamma=\pi/2$. The spectrum at this point is extremely degenerate: Both the continuous and the discrete spectra lie exactly on the imaginary axis. This coincidence accounts for the peculiar simultaneous intersection of curves at the corner in Fig. 2(b).

Now consider the boundary between the locked and unsteady regions. For $K<1$ and for uniform $g(\omega)$, numerics show that locking is lost by a saddle-node bifurcation. This allows us to characterize the boundary analytically—we set $\lambda=0$ in (6) and solve Eqs. (4)-(6) simultaneously. The result[11] for small K is

$$\gamma=\frac{\pi K}{4}\left[1+\frac{K}{6}+\left(\frac{7}{36}-\frac{\pi^2}{64}\right)K^2\right]+O(K^4)\,. \tag{7}$$

Equation (7) generalizes the result $\gamma=\pi K/4$ obtained for phase models,[4] which correspond to the limit $K\to 0$ in Eq. (1). Although Eq. (7) was derived for $K\ll 1$, it agrees with the numerically determined boundary to within 2%, for K as large as 0.8. For $K=1$ and uniform $g(\omega)$, one can prove[11] that the boundary passes through the point $K=1$, $\gamma=\pi/3$. For $K>1$, numerics indicate that the locked state is unique, and so a saddle-node bifurcation is no longer possible; instead locking is lost by a Hopf bifurcation. This part of the boundary is hard to find analytically because one must solve Eqs. (4)-(6) simultaneously with $\mathrm{Re}\lambda=0$ and $\mathrm{Im}\lambda$ to be determined.

Finally, to calculate the boundary between the incoherent and unsteady regions, we determine where another solution branches off the incoherent solution. Specifically, we seek a solution for which (2) is small and *time independent.*[3] As before, we may set $\phi=0$. Then we regard R as a small constant forcing term in (3) and solve for the motion of all the oscillators to $O(R)$. These motions imply a value for R which must be consistent with that assumed. For such a solution the population of oscillators splits into "locked" and "drifting" subpopulations.[14] The self-consistency condition is $R=R_{\text{lock}}+R_{\text{drift}}$. The boundary of the incoherent region is obtained by imposing self-consistency in the limit $R\to 0$.

To find R_{lock}, let $\varepsilon=KR\ll 1$ and $a^2=1-K$. Since all the oscillators satisfy $r=a+O(\varepsilon)$, Eq. (3a) shows that the oscillators with $\omega\le\omega_c=\varepsilon/a+O(\varepsilon^2)$ will lock. Then $\omega=(\varepsilon/a)\sin\theta+O(\varepsilon^2)$ and so

$$R_{\text{lock}}=\int_{-\omega_c}^{\omega_c} r\cos\theta\, g(\omega)\,d\omega=\varepsilon(\pi/2)g(0)+O(\varepsilon^2)\,.$$

To calculate R_{drift}, consider an oscillator of frequency $\omega>\omega_c$. Then Eq. (3) has a stable limit-cycle solution, by the Poincaré-Bendixson theorem. By perturbing around the $\varepsilon=0$ solution $r(t)=a$, $\theta(t)=\omega t+\theta_0$, we find[11] that the path of the limit cycle is $r=a+\varepsilon(A\sin\theta+B\cos\theta)+O(\varepsilon^2)$, where $A=\omega/(\omega^2+4a^4)$ and $B=2a^2/(\omega^2+4a^4)$. To ensure that R_{drift} is time independent, as required by self-consistency, we require that the oscillators of frequency ω form a *stationary* distribution along their limit cycle. Then one can show[11] that these oscillators contribute $\varepsilon B/2+O(\varepsilon^2)$ to R, and hence

$$R_{\text{drift}}=\varepsilon a^2\int_{-\infty}^{\infty}\frac{g(\omega)\,d\omega}{\omega^2+4a^4}+O(\varepsilon^2)\,.$$

By self-consistency, $R=R_{\text{lock}}+R_{\text{drift}}$, and hence a partially synchronized solution branches off the incoherent solution along the curve

$$\frac{1}{K}=\frac{\pi g(0)}{2}+(1-K)\int_{-\infty}^{\infty}\frac{g(\omega)\,d\omega}{\omega^2+4(1-K)^2}\,. \tag{8}$$

In the limit $K\to 0$, Eq. (8) reduces to the result $K=2/\pi g(0)$ obtained for phase models.[1,3] For the uniform distribution, Eq. (8) yields $\tan(2\gamma/K)=2(K-1)/\gamma$, which agrees well with the boundary found numerically. As $K\to 1$, Eq. (8) shows that the boundary ends at $\gamma=\pi/2$, the corner of the death region.

The mean-field model (1) is one of the simplest possible models of coupled nonlinear oscillators, yet it exhibits rich collective behavior. In particular, the long-term behavior of the order parameter can be periodic, quasiperiodic, or chaotic. Such unsteady behavior has not been seen in previous mean-field models of coupled oscillators,[1,3,4,13] but these models were composed of phase-only oscillators. Thus the amplitude degrees of freedom in Eq. (1) may be essential to the unsteady behavior found here.

It is intriguing that oscillators with only two degrees of freedom can cause unsteady behavior. This result persists if $g(\omega)$ is changed to a Gaussian, Lorentzian, or triangle distribution.[11] Beyond its importance for oscillator synchronization, the phenomenon of unsteadiness may have wider implications for the statistical mechanics of nonequilibrium systems. In future studies, one should try to go beyond mean-field theory to consider large systems of limit-cycle oscillators with short-range coupling, and perhaps to extend renormalization-group methods[6,12] to this new class of cooperative systems.

This work is part of an ongoing collaboration with R. E. Mirollo. We thank L. Abbott, C. Marcus, L. Polvani, and S. Yang for helpful conversations. Research supported in part by National Science Foundation Grant No. DMS-8916267 and a Presidential Young Investigator award to S.H.S.

---

[a]Present address: Department of Applied Mathematics and Theoretical Physics, University of Cambridge, Silver Street, Cambridge CB3 9EW, United Kingdom.

[1]A. T. Winfree, J. Theor. Biol. **16**, 15 (1967); *The Geometry of Biological Time* (Springer-Verlag, New York, 1980).

[2]J. Buck, Quart. Rev. Biol. **63**, 265 (1988); T. J. Walker, Science **166**, 891 (1969); D. C. Michaels, E. P. Matyas, and J. Jalife, Circ. Res. **61**, 704 (1987); M. K. McClintock, Nature (London) **229**, 244 (1971).

[3]Y. Kuramoto and I. Nishikawa, J. Stat. Phys. **49**, 569 (1987).

[4]G. B. Ermentrout, J. Math. Biol. **22**, 1 (1985).

[5]H. Sakaguchi, S. Shinomoto, and Y. Kuramoto, Prog. Theor. Phys. **77**, 1005 (1987); S. H. Strogatz and R. E. Mirollo, J. Phys. A **21**, L699 (1988); L. F. Abbott, J. Phys. A (to be published).

[6]H. Daido, Phys. Rev. Lett. **61**, 231 (1988).

[7]Y. Aizawa, Prog. Theor. Phys. **56**, 703 (1976); Y. Yamaguchi and H. Shimizu, Physica (Amsterdam) **11D**, 212 (1984).

[8]M. Shiino and M. Frankowicz, Phys. Lett. A **136**, 103 (1989).

[9]G. B. Ermentrout, Physica (Amsterdam) **41D**, 219 (1990).

[10]R. E. Mirollo and S. H. Strogatz, J. Stat. Phys. **60**, 245 (1990).

[11]P. C. Matthews, R. E. Mirollo, and S. H. Strogatz (to be published).

[12]L. L. Bonilla, Phys. Rev. Lett. **60**, 1398 (1988).

[13]D. S. Fisher, Phys. Rev. B **31**, 1396 (1985); S. H. Strogatz, C. M. Marcus, R. M. Westervelt, and R. E. Mirollo, Phys. Rev. Lett. **61**, 2380 (1988).

[14]Such "partially synchronized" solutions are almost always unstable when $g(\omega)$ is uniform; they are observed numerically only in a tiny region near the lower left corner of the unsteady region. For other $g(\omega)$, partial synchrony can be stable.